Numerical studies of exploding-wire plasmas

David L. Chapin, James J. Duderstadt, and David R. Bach

Department of Nuclear Engineering, The University of Michigan, Ann Arbor, Michigan 48105
(Received 16 October 1972; in final form 13 July 1973)

A plasma created by exploding a thin lithium wire in a vacuum is analyzed using a magnetohydrodynamic (MHD) model. The two-temperature MHD equations including finite thermal conductivity and electrical resistivity are derived in one-dimensional cylindrical geometry. The resulting system of six coupled nonlinear partial differential equations in six unknowns is then solved numerically. Results of the calculation including spatial dependence of density, temperature, and magnetic field and time dependence of the radial profile and average temperature are given. These calculated properties are compared to available experimental results, giving favorable agreement.

I. INTRODUCTION

The method of creating a plasma by discharging an external LC circuit across a thin wire in a vacuum can produce plasmas with greatly varying characteristics. The high current across the wire results in plasmas of high density (10^{18}–10^{20} particles/cm^3) and temperatures ranging from a few eV [1] up to 1 keV, [2] depending on the wire size and material, and the external circuit. These exploding-wire devices are very useful for dense plasma studies and are also of interest in the study of high-density pinch dynamics. For such applications it is important that one know the characteristics of the plasma produced by the exploding wire, particularly such variables as temperature, density, and magnetic field distributions. It is possible to infer some of these variables from diagnostic measurements and by using simple models such as the Bennett relationship and mass conservation. [3] However, such models usually assume infinite electrical conductivity and constant temperature, making them of doubtful validity for low-temperature studies. In this paper we wish to describe detailed numerical one-dimensional magnetohydrodynamic (MHD) calculations of exploding-wire dynamics. The model is described in Secs. II and III, and the predictions of the calculations are compared with available experimental measurements in Sec. IV.

II. MHD MODEL

The MHD model is based on the method of describing the plasma as a hydromagnetic fluid, with separate electron and ion temperatures and both finite thermal conductivity and electrical resistivity. The equations comprising the model are[4,5] (in cgs emu units, temperature in eV):

Ohm's Law

$$\eta\mathbf{J}=\mathbf{E}+\mathbf{u}\times\mathbf{B}; \tag{1}$$

Maxwell's equations,

$$\nabla\times\mathbf{B}=4\pi\mathbf{J}+\frac{1}{c^2}\frac{\partial\mathbf{E}}{\partial t}, \tag{2}$$

$$\nabla\times\mathbf{E}=-\frac{\partial\mathbf{B}}{\partial t}; \tag{3}$$

conservation of mass and momentum,

$$\frac{Dv}{Dt}=v\nabla\cdot\mathbf{u}, \tag{4}$$

$$\frac{D\mathbf{u}}{Dt}=-v\nabla(p_i+p_e)+v\mathbf{J}\times\mathbf{B}; \tag{5}$$

conservation of electron and ion energy,

$$\frac{De_e}{Dt}=-p_e v\nabla\cdot\mathbf{u}+v\nabla\cdot(K_e\nabla T_e)+v\mathbf{J}\cdot(\eta\mathbf{J})-\frac{\partial e_e}{\partial T_e}\frac{(T_e-T_i)}{t_{eq}}, \tag{6}$$

$$\frac{De_i}{Dt}=-p_i v\nabla\cdot\mathbf{u}+v\nabla\cdot(K_i\nabla T_i)+\frac{\partial e_i}{\partial T_i}\frac{(T_e-T_i)}{t_{eq}}, \tag{7}$$

and equations of state ($\alpha=e,i$)

$$e_\alpha=RT_\alpha/(\gamma-1), \tag{8}$$

$$p_\alpha v=RT_\alpha, \tag{9}$$

where

$$\frac{Df(\mathbf{r},t)}{Dt}\equiv\frac{\partial f}{\partial t}+(\mathbf{u}\cdot\nabla)f \tag{10}$$

is the usual Lagrangian or convective time derivative.

Here and elsewhere, η is the resistivity, $\mathbf{J}$ is the current density, $\mathbf{E}$ is the electric field, $\mathbf{B}$ is the magnetic field, $\mathbf{u}$ is the velocity, c is the speed of light, v is the specific volume, p_α, e_α, K_α, and T_α are, respectively, the pressure, internal energy, thermal conductivity, and temperature (in eV) of the electrons ($\alpha=e$) and ions ($\alpha=i$), R is the gas constant, and t_{eq} is the electron-ion equilibration time.

It is now necessary to make some assumptions. First it is assumed that the wave velocity $\mathbf{u}$ is much less than c, so that the displacement current in (2) can be neglected; and in the momentum equation (5), viscous and gravitational forces have been neglected. Also, we have assumed a fully ionized plasma with charge neutrality and no charge separation, so that the ions and electrons move together as a single fluid but with different ion and electron temperatures. Thus there is one velocity $\mathbf{u}$ for both species, and the ion number density n_i is found from

$$n_i=N_0/vA_i, \tag{11}$$

where N_0 is Avogadro's number and A_i is the atomic weight of the ions. Then the electron density $n_e=Zn_i$. Also, we assume the plasma behaves as a polytropic gas so that (8) and (9) are valid. Here γ is the ratio of the specific heats; normally $\gamma=\frac{5}{3}$. The geometry is cylindrical with symmetry in the θ and z directions, so that, neglecting end effects, only radial variations and time dependence are allowed.

Lastly, we choose to describe the plasma in the Lagrangian frame of reference, [6,7] that is, a frame moving with the fluid at velocity $\mathbf{u}$. For this choice the derivative in (10), which is the total time rate of change of the function $f(\mathbf{r},t)$ in this frame, reduces to just $(\partial f/\partial t)_m$, where m is the transformed Lagrangian coordinate defined by

$$m \equiv \int_0^r \frac{r' dr'}{v} = \frac{r^2}{2v}. \quad (12)$$

Thus we see

$$\frac{dm}{dr} = \frac{r}{v} \quad (13)$$

and m is now an independent Lagrangian variable and r becomes a dependent variable. Hence, we now write the system of equations in terms of m. Physically, m is the amount of mass per radian per cm in the plasma. This variable definition is very useful in the numerical solution of the equations, as will be discussed in Sec. III.

Using the geometry described previously, the variables now are $\mathbf{B}=B\hat{\mathbf{e}}_\theta$, $\mathbf{J}=J\hat{\mathbf{e}}_z$, $\mathbf{E}=E\hat{\mathbf{e}}_z$, and $\mathbf{u}=u\hat{\mathbf{e}}_r$, along with the other scalars. To get the magnetic field diffusion equation, substitute (2) in (1) for $\mathbf{J}$ and take the curl, then put (3) in the resulting equation. After expanding the vector products and changing to the Lagrangian frame of reference, we have

$$\left(\frac{\partial B}{\partial t}\right)_m = \frac{\partial}{\partial r}\left(\frac{\eta}{4\pi r}\frac{\partial rB}{\partial r}\right) - B\frac{\partial u}{\partial r}. \quad (14)$$

Note here that the resistivity η is a scalar since $\mathbf{J}$ is perpendicular to $\mathbf{B}$.[8]

To get the electron temperature equation, first rewrite (4) and (6) in the Lagrangian frame and substitute (4) in (6) to obtain (dropping the subscript m on the time derivatives)

$$\frac{\partial e_e}{\partial t} = -p_e\frac{\partial v}{\partial t} + \frac{v}{r}\frac{\partial}{\partial r}\left(rK_e\frac{\partial T_e}{\partial r}\right) + v\eta J^2 - \frac{\partial e_e}{\partial T_e}\frac{(T_e-T_i)}{t_{eq}}. \quad (15)$$

Using (8) to expand $\partial e_e/\partial t$ gives

$$\frac{\partial e_e}{\partial t} = \frac{\partial e_e}{\partial T_e}\frac{\partial T_e}{\partial t} = \frac{R}{\gamma-1}\frac{\partial T_e}{\partial t}, \quad (16)$$

plus (2) and (9) will yield

$$\frac{R}{\gamma-1}\frac{\partial T_e}{\partial t} = -T_e\frac{R}{v}\frac{\partial v}{\partial t} + \frac{v}{r}\frac{\partial}{\partial r}\left(rK_e\frac{\partial T_e}{\partial r}\right) + \frac{v}{(4\pi r^2)^2}\eta\left(\frac{\partial rB}{\partial r}\right)^2 - \frac{R}{\gamma-1}\frac{(T_e-T_i)}{t_{eq}}. \quad (17)$$

A similar equation results for the ion temperature T_i, but without the joule heating term $v\eta J^2$, since the current heats the lighter electrons and then energy is transferred to the ions through the collision term involving t_{eq}.

To complete the set of equations, rewrite (4) and (5) in Lagrangian form, and transform to the new variable m using (13). The resulting equations are

$$\frac{du}{dt} = -r\frac{\partial}{\partial m}\left(\frac{RT_e}{v}\right) - r\frac{\partial}{\partial m}\left(\frac{RT_i}{v}\right) - \frac{B}{4\pi}\frac{\partial rB}{\partial m}, \quad (18)$$

$$u = \frac{dr}{dt}, \quad (19)$$

$$\frac{dv}{dt} = \frac{\partial ru}{\partial m}, \quad (20)$$

$$\frac{\partial B}{\partial t} = \frac{r}{v}\frac{\partial}{\partial m}\left(\frac{\eta}{4\pi r}\frac{\partial rB}{\partial r}\right) - B\frac{r}{v}\frac{\partial u}{\partial m}, \quad (21)$$

$$\frac{R}{\gamma-1}\frac{\partial T_e}{\partial t} = -T_e\frac{R}{v}\frac{\partial v}{\partial t} + \frac{\partial}{\partial m}\left(rK_e\frac{\partial T_e}{\partial r}\right) + \frac{v}{(4\pi r^2)^2}\eta\left(\frac{\partial rB}{\partial r}\right)^2 - \frac{R}{\gamma-1}\frac{(T_e-T_i)}{t_{eq}}, \quad (22)$$

$$\frac{R}{\gamma-1}\frac{\partial T_i}{\partial t} = -T_i\frac{R}{v}\frac{\partial v}{\partial t} + \frac{\partial}{\partial m}\left(rK_i\frac{\partial T_i}{\partial r}\right) + \frac{R}{\gamma-1}\frac{(T_e-T_i)}{t_{eq}}. \quad (23)$$

Equations (18)–(23) comprise the set of MHD equations for six variables: u, r, v, B, T_e, and T_i. The second equation, which is just the definition of the velocity, is necessary to complete the model. The forms for the equilibration time t_{eq} and resistivity η are from Spitzer,[8] while the forms for the electron and ion thermal conductivities K_e and K_i are taken from Braginskii.[9]

III. NUMERICAL SOLUTION

Equations (18)–(23) represent a set of six nonlinear coupled partial differential equations in six unknowns. The equations were solved numerically in a manner similar to the methods of Refs. 5 and 10. The scheme entailed dividing the plasma into N concentric circles or zones and then finite differencing the equations,[11] using an implicit numerical solution to find B, T_e, and T_i, and an explicit solution to find u, r, and v. The variables v, B, T_e, and T_i are calculated at the midpoint of each zone, while u and r are calculated at the boundary of each zone.

To begin the calculations, various initial and boundary conditions are given to the code. These include the initial and boundary temperatures T_e and T_i, initial radius and density, the atomic weight of the ions, and N, the number of zones. It is also necessary to know the value of the axial current flowing through the plasma so that the magnetic field on the boundary can be calculated. This could be numerically calculated at each time step from the parameters of the external circuit. However, since the circuit we utilized provided essentially just a short circuit across the wire, the current used in the code is of the form

$$I(t) = \exp(-\alpha t) I_0 \sin\omega t, \quad (24)$$

where α, I_0, and ω are input values.

The code begins by dividing the plasma into N radial zones of equal spacing. Then Δm, the mass in each zone per centimeter per radian, is calculated from the finite difference form of (13). This Δm then remains constant at the initial values as the code is run, hence becoming an independent variable. The basic steps of the procedure are first to calculate the velocity u from (18), then calculate the radius r from (19), and the specific volume v from (20). Equations (21)–(23) are next solved to find B, T_e, and T_i. Then the variables are shifted and the algorithm repeats, calculating new values in terms of the previous ones. The time steps Δt are not constant but instead are allowed to vary subject to constraints.

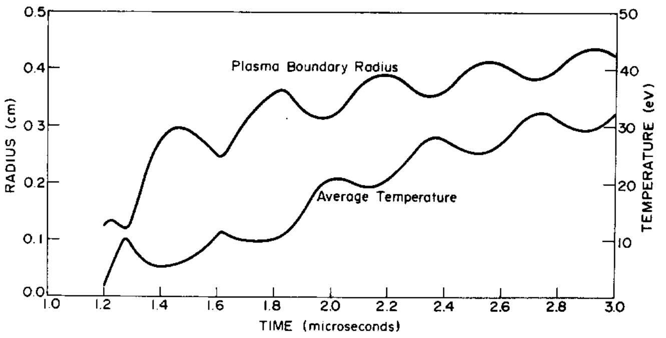

FIG. 1. Calculated plasma front trajectory and density averaged temperature as functions of time.

These limits involve the change in certain variables from one time step to the next, and also the condition that Δt must be less than the time for a magnetosonic wave[4,8] to travel across a zone. Thus, if the variables are changing slowly the time step may be increased, resulting in shorter run times for the code. Also, to prevent discontinuities in the region of shocks during the numerical calculation, the usual Richtmyer-Von Neumann artificial viscosity[11,12] is added to the ion temperature equation (23) and the momentum equation (18).

Since this model did not contain ionization dynamics, it was not possible to investigate the exploding wire at

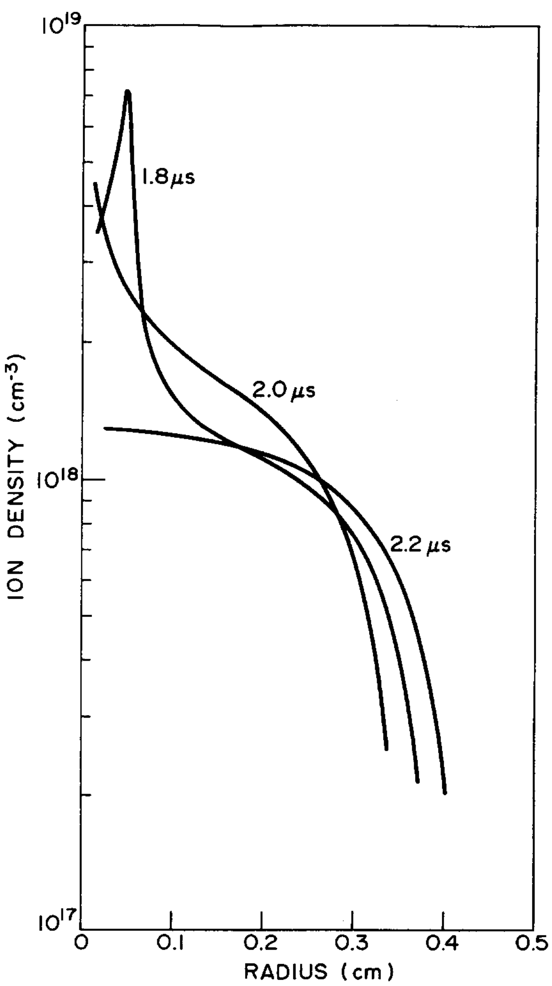

FIG. 2. Calculated ion density profiles vs radius at three different times: 1.8, 2.0, and 2.2 μ-sec.

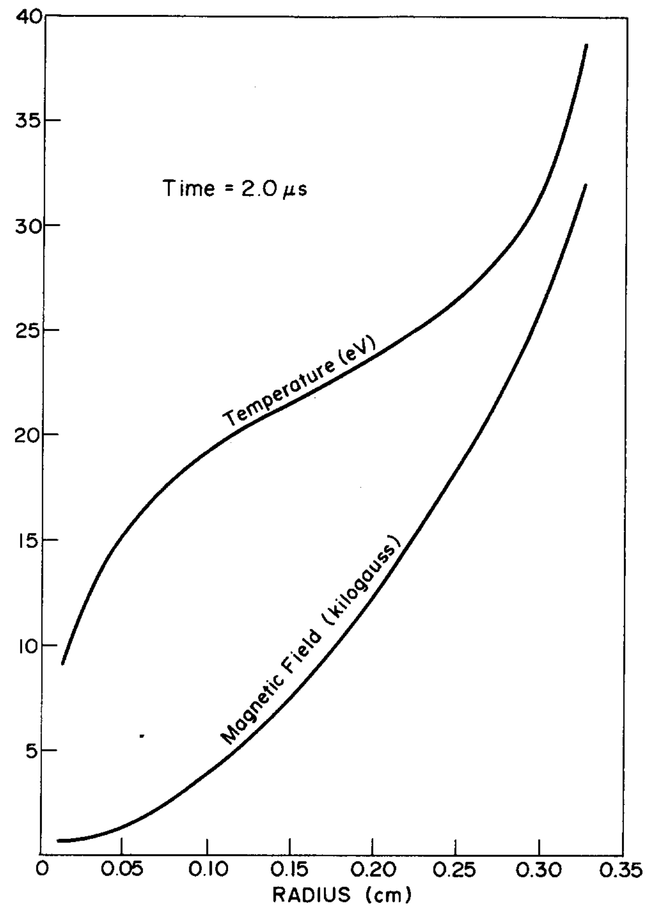

FIG. 3. Calculated temperature and magnetic field profiles vs radius at time 2.0 μ-sec.

early times. Instead studies were initiated at some later time after the wire had been exploded and a fully ionized plasma had been formed. The experiment utilized lithium wires, and experimental measurements and theoretical calculations[1] show that shortly after explosion the plasma was fully ionized with the lithium ions being either singly or doubly ionized.

IV. EXPLODING-WIRE ANALYSIS

The experiment under investigation consisted of extruding a thin lithium wire, 25–50 μ in diameter and 5 cm in length, in a vacuum chamber at 5×10^{-5} Torr. A high-voltage source of 15 kV was used to charge up a 14-μF low-inductance capacitor, which was then discharged by triggering a spark gap switch. The current produced across the wire was measured to be of the form of (24), with a peak current of $I_0 = 10^5$ A occurring at 3.5 μsec. Streak photographs of the plasma radius versus time show that the plasma is strongly pinched until it is disrupted by instabilities at about 3 μsec.

The MHD calculations were initiated 1.2 μsec after the triggering of the spark gap, since the time range 1.5–3.0 μsec was the most interesting interval as far as the experimental studies were concerned. The radial mesh was divided into 45 zones ($N=45$) and typical time steps were 1–5 nsec. From the streak photographs, the plasma diameter was found to be ~2.5 mm, 1.2 μsec after the initial discharge. Knowing the approximate diameter of the solid wire, the plasma density at 1.2 μsec was calculated to be $\sim 9.0\times 10^{18}$ using particle conservation. The initial electron and ion temperatures were assumed to be 1 eV. The following discussion of results is for the analysis using these initial conditions of density, diameter, and temperature.

Figure 1 shows the outer radius R_0 of the plasma and the density averaged temperature $\langle T\rangle$ versus time, where $\langle T\rangle$ is found from numerical integration of

$$\langle T\rangle \equiv \int_0^{R_0} n_i T\,dr \left(\int_0^{R_0} n_i\,dr\right)^{-1}. \qquad (25)$$

In (25) it does not matter whether the electron or ion temperature is used because they are nearly identical, due to the short equilibration times (on the order of nanoseconds) for these densities and temperatures.

In Fig. 1, the pinching of the plasma is clearly indicated, with four bounces occurring in the calculated front trajectory. This is in good agreement with streak photographs of the radial profile, which show similiar pinching and bouncing. These streak photographs also show a pattern of each peak in the profile being slightly larger than the previous one, again in agreement with the calculated profile. Also in Fig. 1, the plot of the average temperature $\langle T\rangle$ shows peaks corresponding to the pinching of the plasma, due to heating by compression. When expansion then occurs the temperature drops slightly, as expected. However, $\langle T\rangle$ is over all an increasing function with time, due to the constantly increasing current which produces increasing joule heating effects. Average temperatures of slightly over 30 eV are found near the end of the calculation, when the plasma has expanded to nearly $\frac{1}{2}$ cm.

In Fig. 2, the variation of ion density with radius is shown for three different times. Note that at 1.8 μsec a peak is shown near the center of the plasma, but at later times the profile becomes smooth. This peak at the early time results from the initial condition of using a constant density profile. Typical ion densities are shown to be in the range $5\times 10^{18}-2\times 10^{17}/\text{cm}^3$. For the calculated temperatures at these times from Fig. 1, the lithium ions are mainly singly ionized, resulting in equal electron and ion densities.

Figure 3 shows the temperature (electron or ion) and magnetic field as a function of radius at 2.0 μsec. Both profiles are found to be smooth increasing functions of radius; and plots of these variables at other times yield similiar shapes. The temperature varies from 9 eV at the center of the plasma to nearly 40 eV at the boundary, which gives a $\langle T\rangle$ from (25) of 18.9 eV, due to the higher density near the center. The magnetic field varies from 600 G at the center to 32 kG at the boundary. Using the values of n, T, and B from Figs. 2 and 3 at 2.0 μsec, the parameter β is found to be greater than 1.0, where β is the ratio of the plasma kinetic pressure from (9) to the pressure exerted by the magnetic field. If β is greater than 1.0, then the plasma should be expanding, as can be seen from Fig. 1 at 2.0 μsec.

One of the main purposes of the experiment is to measure the absorption of electromagnetic radiation incident on the plasma. Since the absorption coefficient depends on density and temperature,[13] it can be calculated using the results of the MHD code. The agreement between the calculated and experimentally determined absorption coefficients assuming inverse bremsstrahlung processes is very good, providing a check on the results of the model.

In conclusion, it appears that the predictions of this MHD model of an exploding-wire plasma are consistent with experimental measurements. The calculated front trajectory and absorption coefficients are in agreement with results of the experiment. It is hoped that this computational model will prove useful in analyzing and extrapolating further measurements performed on the plasma.

[1]T.A. Leonard and D.R. Bach, J. Appl. Phys. **44**, 2555 (1973).
[2]S.J. Stephanakis, L.S. Levine, D. Mosher, I.M. Vitkovitsky, and F. Young, Phys. Rev. Lett. **29**, 568 (1972).
[3]S. Glasstone and R.H. Lovberg, *Controlled Thermonuclear Reactions* (Van Nostrand, Princeton, New Jersey, 1960).
[4]A.B. Cambel, *Plasma Physics and Magnetofluidmechanics* (McGraw-Hill, New York, 1963).
[5]K.V. Roberts and D.E. Potter, in *Methods in Computational Physics*, edited by B. Alder, S. Fernbacg, and M. Rotenberg (Academic, New York, 1970), Vol. 9.
[6]Y.B. Zel'dovich and Y.P. Raizer, *Physics of Shock Waves and High-Temperature Hydrodynamic Phenomena* (Academic, New York, 1966), Vol. 1.
[7]J.D. Jackson, *Classical Electrodynamics* (Wiley, New York, 1962).
[8]L. Spitzer, Jr., *Physics of Fully Ionized Gases*, 2nd ed. (Interscience, New York, 1962).
[9]S.J. Braginskii, *Reviews of Plasma Physics* (Consultants Bureau, New York, 1965), Vol. 1.
[10]K. Hain, G. Hain, K.V. Roberts, S.J. Roberts, and W. Koppendorfer, Z. Naturforsch. A **15**, 1039 (1960).
[11]R.D. Richtmyer and K.W. Morton, *Difference Methods for Initial Value Problems*, 2nd ed. (Interscience, New York, 1967).
[12]J. VonNeumann and R.D. Richtmyer, J. Appl. Phys. **21**, 232 (1950).
[13]T.W. Johnston and J.M. Dawson, Phys. Fluids **16**, 722 (1973).